www.czasopisma.pan.pl PAN www.journals.pan.pl
Opto-Electronics Review 27 (2019) 137–142

Contents lists available at ScienceDirect

Opto-Electronics Review

journal homepage: http://www.journals.elsevier.com/opto-electronics review

A solution-processable small-organic molecules containing carbazole or phenoxazine structure as hole-transport materials for perovskite solar cells

K. Gawlińska-Nęcek[a], Z. Starowicz[a], D. Tavgeniene[b], G. Krucaite[b], S. Grigalevicius[b], E. Schab-Balcerzak[c], M. Lipiński[a,*]

[a] Institute of Metallurgy and Materials Science, Polish Academy of Sciences, Reymonta 25 St., 30-059, Krakow, Poland
[b] Department of Polymer Chemistry and Technology, Kaunas University of Technology, Radvilenu Plentas 19, LT50254, Kaunas, Lithuania
[c] Institute of Chemistry, University of Silesia, 9 Szkolna St., 40-006, Katowice, Poland

ARTICLE INFO

Article history:
Received 6 March 2019
Received in revised form 17 April 2019
Accepted 26 April 2019
Available online 24 May 2019

Keywords:
Carbazole derivatives
Perovskite photovoltaic cells
Hole transporting materials

ABSTRACT

Three low molecular weight compounds bearing carbazole units (1,6-di{3-[2-(4-methylphenyl)vinyl]carbazol-9-yl}hexane and 9,9'-di{6-[3-(2-(4-methylphenyl)vinyl)-9-carbazol-9-yl]hexyl}-[3,3']bicarbazole) and phenoxazine structure (10-butyl-3,7-diphenylphenoxazine) were tested as hole-transporting materials in perovskite solar cells. Two of them were successfully applied as hole transporting layers in electroluminescent light emitted diodes. The examined compounds were high-thermally stable with decomposition temperature found at the range of 280–419 °C. Additionally, DSC measurement revealed that they can be converted into amorphous materials. The compounds possess adequate ionization potentials, to perovskite energy levels, being in the range of 5.15–5.36 eV. The significant increase in power conversion efficiency from 1.60% in the case of a device without hole-transporting layer, to 5.31% for device with 1,6-di{3-[2-(4-methylphenyl)vinyl]carbazol-9- yl}hexane was observed.

1. Introduction

Since, 2012 when the first all-solid-state perovskite solar cell with power conversion efficiency (PCE) about 9% has been obtained, the significant progress in their PCE is observed [1,2]. The hole-transporting layer in such type of photovoltaic cell plays an important role in facilitating charge separation and transportation, recombination reduction at the interface and tuning the work function of the electrode leading to increasing of PCE [3–5]. In the literature, a lot of examples of organic [6–9] and inorganic [10,11] compounds as hole-transporting materials (HTM) were described. Among them, low molecular weight compounds dominate. The advantages of small molecules are their well-defined structure, which transpose into the efficient and reproducible synthesis of compounds with high purity, even in industrial conditions, compared to polymeric materials. In addition, the appropriate change of functional groups or replacement of substituents allows for modification of some properties (electrochemical, optical, and solubility) of the final derivatives. The most popular as HTM materials in PSC is 2,2′,7,7′-tetrakis (*N,N*-di-p-methoxyphenylamine)-9,9′-spirobifluorene (Spiro-OMeTAD), which PCE values exceed 20% [4–7]. However, despite the many advantages of Spiro-OMeTAD the design and synthesis of efficient HTMs is an important research topic [12]. The major drawbacks of Spiro-OMeTAD molecule are high cost, complicated and long both synthesis and purification [3]. Moreover, there are the ever-growing requirements regarding the transport of holes, blocking electron flow, stability, solubility, and resistance to the impact of the external environment for HTMs [12]. Thus, despite the efforts which have been made for the development of alternative HTMs, the challenges related to looking for a new one is still existing.

The aim of our work was testing implementation of selected compounds consisting of carbazole or phenoxazine units, in perovskite solar cells. Two of them, that is, 1,6-di{3-[2-(4-methylphenyl)vinyl]carbazol-9-yl}hexane and 10-butyl-3,7-diphenylphenoxazine were successively applied as HTM in OLEDs [13,14]. The third tested compound that is, 9,9'-di{6-[3-(2-(4-methylphenyl)vinyl)-9-carbazol-9-yl]hexyl}-[3,3']bicarbazole has not been described in the literature yet.

* Corresponding author.
E-mail address: m.lipinski@imim.pl (M. Lipiński).

https://doi.org/10.1016/j.opelre.2019.04.003
1230-3402/

2. Experimental

2.1. Synthesis of 9,9'-di{6-[3-(2-(4-methylphenyl)vinyl)-9-carbazol-9-yl]hexyl}-[3,3']bicarbazole (**2**)

A 9,9'-di{6-[3-(2-(4-methylphenyl)vinyl)-9-carbazol-9-yl]hexyl}-[3,3']bicarbazole (**2**) was prepared by multistep synthetic route, which is demonstrated in Scheme 1.

Starting materials for the synthesis, i.e. 9H-carbazole (**2.1** in Scheme 1), 1,6-dibromohexane, iron (III) chloride ($FeCl_3$), potassium hydroxide (KOH), phosphorus trichloride ($POCl_3$), dimethylformamide (DMF), tetra-n-butylammonium hydrogen sulfate (TBAHS), potassium *tert*-butoxide (*t*-BuOK) and diethyl-4-methylbenzylphosphonate were purchased from Aldrich and used as received.

A 9H,9'H-[3,3']-bicarbazole (**2.2** in Scheme 1) was synthesized according to the our earlier described procedure [15].

A 9-(6-Bromohexyl)carbazole (**2.3** in Scheme 1) was synthesized according to the procedure described in literature [16].

A 9-(6-Bromohexyl)-3-formylcarbazole (**2.4**) was also synthesized according to the procedure described in literature [17].

A 9,9'-Di[6-(3-formylcarbazol-9-yl)hexyl]-[3,3']bicarbazole (**2.5**) was prepared by the reaction of 9H,9'H-[3,3']-bicarbazole (**2.2**) with excess of 9-(6-bromohexyl)-3-formylcarbazole (**2.4**) under basic conditions in the presence of TBAHS phase transfer catalyst. 1.0 g (3.0 mmol) of the compound **2.2** and 2.36 g (6.6 mmol) of compound **2.4** were heated to reflux in 60 ml of THF. Then 1.02 g (18.2 mmol) of powdered KOH and a catalytic amount of TBAHS were added to the mixture, and it was refluxed for 4 h. After TLC control the mixture was filtered, the solvent was evaporated. The product was purified by column chromatography with silica gel using ethyl acetate/hexane (vol. ratio 1:4) as an eluent. Yield: 1.5 g (56%) of yellow amorphous material with glass transition temperature of 110 °C (DSC).

HRMS: Found $[M+H]^+$ 887.1145; molecular formula $C_{62}H_{54}N_4O_2$ requires $[M+H]^+$887.1156; ^{1}H NMR (400 MHz, $CDCl_3$): 9.96 (s, 2H, 2 × CHO), 8.30 (s, 2 H, Ar), 8.13–8.00 (m, 4H, Ar), 7.84 (dd, 2H, J_1 = 1.6 Hz, J_2 = 8.8 Hz, Ar), 7.67 (dd, 2H, J_1 = 1.6 Hz, J_2 = 8.4 Hz, Ar), 7.43–7.42 (m, 7H, Ar), 7.25–7.13 (m, 8H, Ar), 4.19 (t, 4H, J = 7.2 Hz, 2×NCH_2), 4.14 (t, 4H, J = 7.2 Hz, 2×NCH_2), 1.81–1.70 (m, 8H, 4×NCH_2CH_2), 1.33–1.30 (m, 8H, 4×$NCH_2CH_2CH_2$). ^{13}C NMR (400 MHz, $CDCl_3$): 191.78, 143.99, 141.08, 140.84, 139.49, 133.34, 128.52, 127.25, 126.75, 125.75, 125.53, 123.91, 123.44, 123.06, 122.98, 120.77, 120.52, 120.34, 118.94, 118.91, 109.33, 108.85, 108.83, 108.72, 43.14, 42.91, 28.89, 28.76, 27.05, 27.02. FT-IR (KBr), cm^{-1}: 3050, 2928, 2877, 2863, 2723, 1733, 1679, 1626, 1591, 1481, 1385, 1328, 1236, 1134, 892, 799, 767, 744, 727.

A 9,9'-Di{6-[3-(2-(4-methylphenyl)vinyl)-9-carbazol-9-yl]hexyl}-[3,3']bicarbazole (**2**) was prepared by the reaction of compound **2.5** with an excess of diethyl-4-methylbenzylphosphonate in dry THF. 0.33 g (3.4 mmol) *t*-BuOK and 15 ml dry THF were placed in a flask at room temperature under nitrogen atmosphere. 0.33 g (2.3 mmol) of diethyl-4-methylbenzylphosphonate was added dropwise to the THF solution at 0 °C under nitrogen. The reaction mixture was stirred for 20 min. Then, 0.5 g (0.6 mmol) of the compound **2.5** was added to the reaction mixture. The resulting solution was stirred at room temperature under the basic conditions for 3 h, until the starting compound **2.5** reacted completely. Then, the mixture was poured into ice water and extracted by chloroform. Organic fraction was dried by Na_2SO_4 and the solvent was removed by evaporation. The product was purified by column chromatography with silica gel using ethyl acetate/hexane (vol. ratio 1:7) as an eluent. Yield: 0.3 g (50%) of yellow crystals. M.p.: 119 °C (DSC). HRMS: Found: $[M+H]^+$ 1063.4132; molecular formula $C_{78}H_{70}N_4$ requires $[M+H]^+$1063.4144; ^{1}H NMR (400 MHz, $CDCl_3$,): 8.31 (s, 2 H, Ar), 8.16–8.08 (m, 3H, Ar), 8.03 (d, 2H, J = 7.6 Hz, Ar), 7.67 (dd, 2H, J_1 = 2.0 Hz, J_2 = 8.4 Hz, Ar), 7.51 (dd, 2H, J_1 = 1.6 Hz, J_2 = 8.4 Hz, Ar), 7.40–7.19 (m, 15H, Ar), 7.17–6.98 (m, 10H, Ar, 2×CH = CH), 4.26–4.07 (m, 8H, 4×NCH_2), 2.28 (s, 6H, 2×CH_3), 1.85–1.70 (m, 8H, 4×NCH_2CH_2), 1.62–1.54 (m, 4H, 2×$NCH_2CH_2CH_2$), 1.33–1.30 (m, 4H, 2×$NCH_2CH_2CH_2$). ^{13}C NMR (400 MHz, $CDCl_3$,): 140.84, 140.77, 140.08, 139.50, 136.77, 135.18, 133.37, 129.36, 128.76, 128.63, 126.13, 126.01, 125.79, 125.69, 125.59, 124.41, 123.41, 123.18, 123.08, 122.90, 120.50, 120.46, 119.01, 118.93, 118.83, 118.52, 108.84, 108.79, 108.72, 42.90, 28.85, 28.82, 27.03, 21.24. FT-IR (KBr), cm^{-1}: 3046, 3020, 2926, 2853, 1625, 1598, 1487, 1471, 1378, 1345, 1331, 1238, 1153, 959, 810, 792, 746, 723.

2.2. Devices preparation

The FTO (fluorine-doped tin oxide, Solaronix) substrates were cleaned for 5 min in worm deionized water (DI H_2O) with detergent and 5 min in isopropanol (POCH) in an ultrasonic bath. The titanium oxide blocking layer was prepared by sol-gel method. A solution of TiO_2 was a mixture of 50 ml of ethanol (96%, POCH) with 1 ml of HCl (36%, CHEMPUR) and 25 mM titanium (IV) ethoxide ($Ti(OC_2H_5)_4$) from Merck. The blocking layer was deposited on a glass substrate with FTO by spin coating method at 2000 rpm for 15 s. Subsequently, substrates were dried at 200 °C for 10 min and annealed at 500 °C for 30 min in the oxygen atmosphere. Analogically, the layers on polished silicon wafers were deposited for other measurement purposes. Mesoporous titanium dioxide layer was deposited on top of the blocking layer from dilutes TiO_2 paste (Solaronix 600) by spin-coater at 2000 rpm for 15 s. The dilution was a mixture of 0.865 g of paste and 3 ml of anhydrous ethanol (POCH). To prepare the perovskite layer two-step deposition method was used. Lead iodide solution was prepared by mixing 1.39 g perovskite grade PbI_2 (Sigma-Aldrich) with 3 ml of anhydrous DMF (Sigma-Aldrich) and hitting 70 °C 30 min with stirring. Subsequently, PbI_2 was spin-coated on cleaned FTO substrates with 2000 rpm. for the 30 s and dried at 70 °C for 3 min and at 90 °C for 5 min. Next step was 5 min immersing in methylammonium iodide solution which was prepared from 0.1 g MAI (Solaronix) and 10 ml IPA (Chempur) and drying at 90 °C for 30 min. The tested compounds solutions were obtained by mixing 7×10^{-5}, 1.7×10^{-5} and 1.2×10^{-4} mole of **1**, and **3** in 1 ml of chlorobenzene (Chempur), respectively. All tested HTM's were doped by 39 µl 4-tBP (Sigma-Aldrich) and 18 µl LiTFSI (Sigma-Aldrich) in acetonitrile (Archem) and were deposited on the top of perovskite by using spin coater at 2000 rpm for 30 s. Finally, gold back electrode was evaporated.

2.3. Measurements

Photovoltaic performances measurements were carried out by I-V curve tracing using PET Photo Emission Tech AAA class solar simulator under STC conditions. The optical characterization of compounds on BK7 glass was carried out using ellipsometry (ellipsometer Sentech SE800 PV) and UV-VIS-NIR (spectrophotometer Lambda 950S) spectroscopy measurements. The perovskite morphology with or without HTM was visualized by atomic force microscope (AFM). The planar heterojunction-based perovskite solar cells were simulated with the program SCAPS 3.3.05 [18]. Values of Td of the materials were appointed by thermo-gravimetric analysis (TGA). The TGA measurements were performed on a Netzsch STA 409 in a nitrogen atmosphere at a heating rate of 10 °C/min. The ionization potentials (Ip) were measured using the electron photoemission method. The electron photoemission method for measurement of ionization potentials (Ip) of the solid-state layers of the studied compounds was exploited in air [19]. The

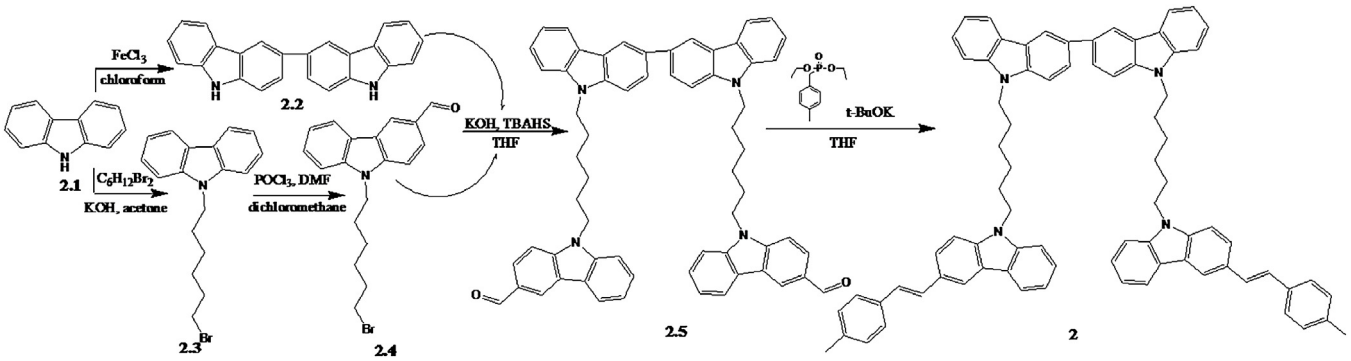

Scheme 1. Multistep synthetic route of the investigated compound **2**.

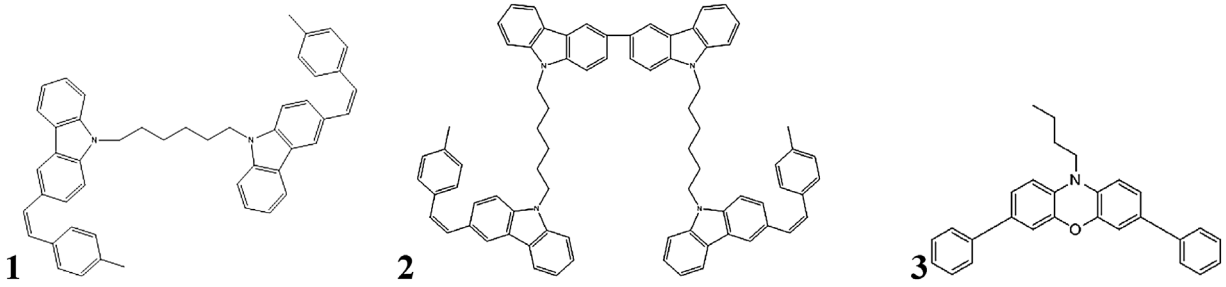

Fig. 1. The chemical structure of the investigated compounds.

experimental setup was similar as we have previously described [20].

3. Results and discussion

The chemical structure of the compounds employed as HTM in perovskite solar cells is depicted in Fig. 1.

The ideal HTMs should fulfill certain requirements concerns their properties. It is expected that efficient HTMs will be exhibiting well aligned highest occupied molecular orbital energy level (HOMO) with the valence band energy of the perovskite, minimal absorption in the region of the solar spectrum, high hole mobility, sufficient thermal and photo-stability. Of much significance is also the cost of its synthesis [5]. The investigated herein compounds showed high thermal stability with decomposition temperature (T_d) at 419 °C, 398 °C and 280 °C for **1**, **2** and **3**, respectively [13,14]. They were obtained as crystalline solids with melting temperature at 176 °C for **1**, 119 °C for **2** and 101 °C for **3** DSC measurements revealed that they can be converted to amorphous state with a glass transition temperature (T_g) in the range of 119 (**1**) – 84 (**2**) – 53 °C (**3**). The high T_g gives the possibility for preparation of morphologically-stable amorphous films. Ionization potential (IP) of studied compounds, which is closely related to the energy levels of the HOMO is compatible with perovskite (cf. Fig. 2). The good fit of the energy levels should lead to the efficient transport of holes generated in the photovoltaic conversion process.

The IP of compounds bearing carbazole units (**1** and **2**) is slightly higher than that of $MAPbI_3$ contrary to a molecule with phenoxazine structure (**3**). Hole drift mobility values exceeding 9.2×10^{-5} $cm^2V^{-1}s^{-1}$ were observed in amorphous layers of these hole transporting materials at an electric field of 4×10^5 Vcm^{-1} at 25 °C as it was established by time-of-flight (ToF) measurements [14]. The optical properties of **1**, **2** and **3** in the form of a film on glass substrate were analyzed by UV–vis spectroscopy and their transmission spectra are depicted in Fig. 3.

The tested materials absorb the radiation in the range from above 250–400 nm. Compound with two carbazole units (**2**) exhibited absorption up to 300 nm contrary to the others (**1** and **3**), which absorption is bathochromically shifted to lower energy region to ca. 360 nm. Interestingly, all of the tested materials presented a characteristic slop located at 310 −320 nm. The investigated compounds showed the optical band gap (E_g) derived from the Tauc plot in the range of 2.86–3.14 eV. The introduction of the phenoxazine unit (**3**) lowered the E_g to 2.86 eV. Together with decease of carbazole units number (**1**) the increase of E_g to 3.14 eV was observed. Based on E_g and IP values, the electron affinity values (corresponded to LUMO levels) were calculated being 2.01, 2.22 and 2.49 eV for **1**, **2** and **3**, respectively. It can be noticed that all of the proposed materials fit into the energy structure of the perovskite solar cell and were utilized for the fabrication of a device with structure presented in Fig. 2.

Before focusing on photovoltaic measurements of the prepared PSCs, the perovskite morphology without and with HTMs seem to be important for discussion. Representative AFM images recorded for perovskites are presented in Fig. 4.

It was found that in the case of the perovskite not covered by any HTM large, sharpened crystals were observed. The average Ra was 65.6 nm and ΔZ ~400 nm. While, for perovskite covered with molecule **2**, HTM cannot be distinguished on the topography as well as the phase, while smaller crystals and clearly lower roughness were observed. The average Ra is 45.7 nm and ΔZ ~200 nm. The Ra reduction is evidently indicative of the presence of the HTM layer on the perovskite. It is very interesting how the additional layer influenced the shape of perovskite grains, which were reduced. It should be emphasized that HTM locates in the space between the grains, thus the grains appear smaller, their shapes less sharp and Ra decreases. An ellipsometric study performed on silicon indicated that the thickness of the organic layer prepared from molecule **2** was 40–55 nm.

For a thorough understanding, of the role of HTM in perovskite solar cells, the simulation was carried out using the program SCAPS 3.3.05. Some parameters of HTM were experimentally determined (ionization potential, optical bandgap, electron affinity). Others parameters like mobility, acceptor concentration were

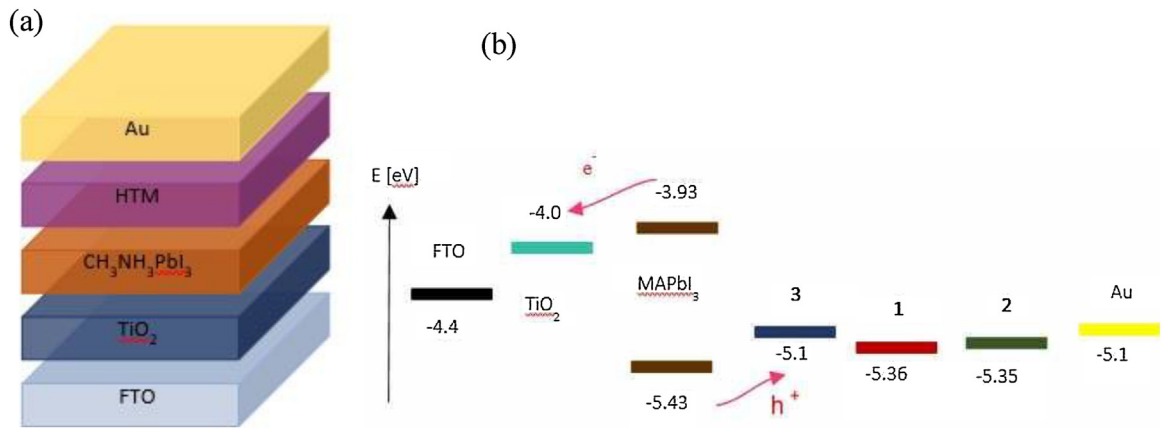

Fig. 2. Device scheme (a) and energy levels diagram (b) of the fabricated PSCs.

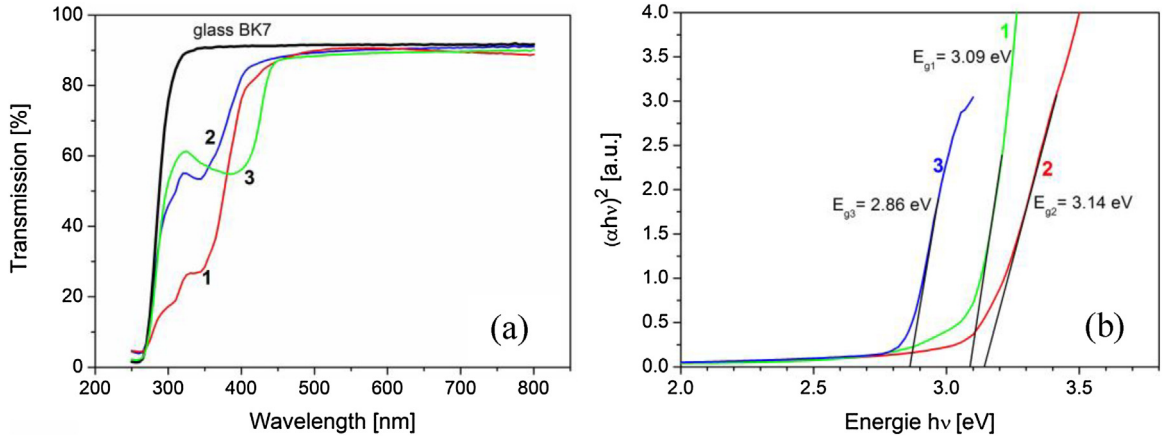

Fig. 3. UV–vis transmission spectra of the investigated HTMs deposited on the glass (a) and optical band gap (b) of the HTMs estimated from Tauc plot.

adopted as for Spiro-OMeTad from literature [21]. Additionally, some assumption was made in order to obtain more realistic parameters of cells similar to those manufactured in our laboratory: Shockley–Read–Hall (SRH) recombination was included in such way as to obtain the carrier diffusion about 120 nm. It was assumed that the series resistance is equal to 10 $\Omega \times cm^2$, the parallel resistance 1 k $\Omega \times cm^2$ and the FTO glass transmission 90%. Simulation results show an important role that HTM plays (Fig. 5).

Although it is possible to make cells without HTM, their efficiency is significantly smaller in comparison to the device with HTM [Fig. 5(a)]. Fig. 5(a) shows that efficiencies for **1** and **3** are higher than for **1** and Spiro-OMeTAD, as well. All tested HTMs improve the efficiency in comparison with the cell without HTM. Photovoltaic parameters of the fabricated devices were obtained based on registered current-voltage (I-V) characteristics, which are given in Fig. 6.

Current-voltage curves indicate a lower fill factor (FF) for all new HTM's compared to device with Spiro-OMeTAD. The curves slope is evident on both, large series resistance R_s and low shunt resistance R_{sh}. The photovoltaic parameters of the prepared cells has been gathered in Table 1.

It is worth noting that all of the tested HTMs improved the open circuit voltage (V_{oc}) with respect to the reference cell without HTM. A reference cell (without HTM) showed a short-circuit current of 1.99 mA and 0.64 V open circuit voltage with a value of fill factor slightly higher than 40%, which makes the efficiency equal to 1.6%. That is an effect of increased recombination in the solar cell due to the lack of effective charge separation caused by the absence of HTM. For a device with compound **1** and **3,** the lowest J_{sc} was

Table 1
Photovoltaic parameters of the studied PSCs.

HTM	I_{sc} [mA]	J_{sc} [mA/cm^2]	V_{oc} [mV]	FF [%]	PCE [%]
1	0.99	3.96	917	36.9	1.32
2	4.39	17.56	869	35.2	5.31
3	1.10	4.40	747	34.4	1.11
Spiro-OMeTAD	4.46	17.84	974	58.0	9.98
without HTM	1.99	7.96	641	.41.0	1.60

obtained. An interesting fact is an increase in voltage of 0.75 V for **3** and 0.92 V for **1**. This proves low voltage losses on the junction. Nevertheless, due to the low short circuit current of the cell with the **1** and **3** layer, the final efficiency is lower than the reference device without HTM. The best performances among tested materials were obtained for the cell where **2** was employed. Such device was characterized by the highest short-circuit current of 4.39 mA and good voltage of 0.87 V. However, similar to the other tested materials, fill factor, was lower of approximately 35%. As can be presumed from the analysis of the electrical parameters of the solar cells, the low fill factor is associated with an increase of series resistance which results from a slightly low short-circuit current. The low value of this parameter is certainly a consequence of the isolating nature of the applied HTM. The voltage is likewise lower which is related to poor parallel resistance and charge leakage. Nevertheless, if the conductivity of compound **2** could be improved by appropriate doping causing probably that the fill factor and cell parameters would increase. What interesting control device with **2** without any doping presented quite similar electrical parameters compared with doped **2**. The open circuit voltage was 0.87 V, short circuit current

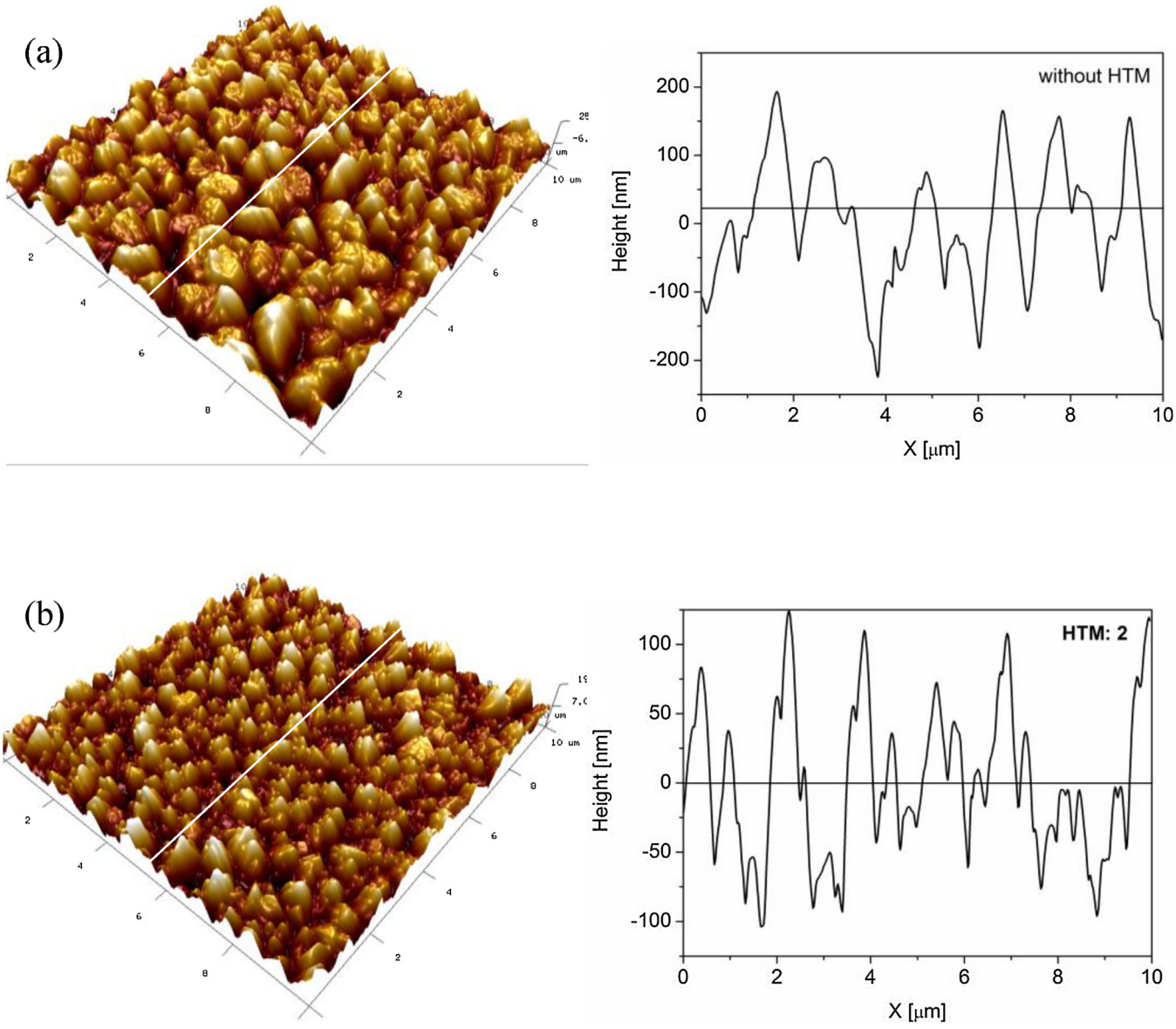

Fig. 4. AFM images of perovskite surfaces: (a) without HTM and (b) covered with compound **2**.

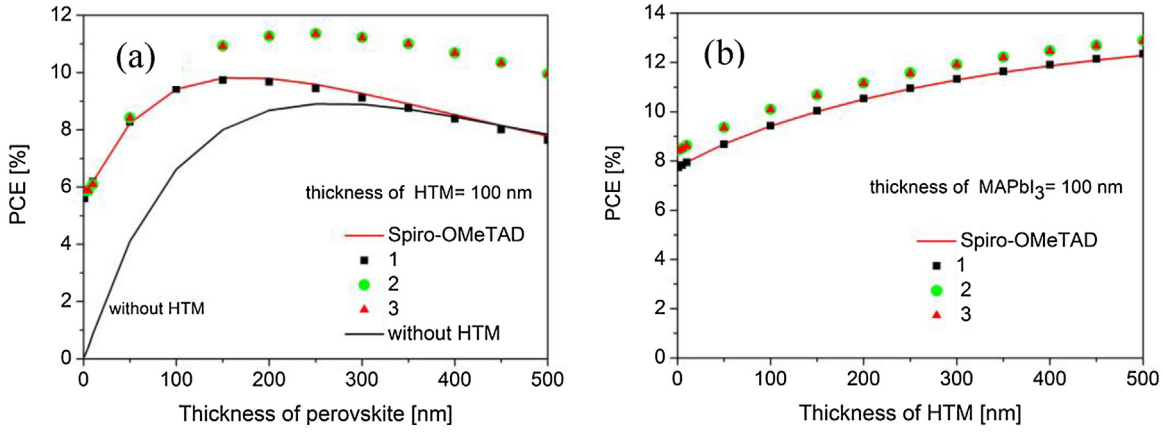

Fig. 5. Results of simulation of perovskite solar cells with HTMs **1**, **2**, **3**, Spiro-OMeTAD (for thickness of HTM equal to 100 nm) and without HTM for different thickness of perovskite layer (a) and HTM layer for thickness of perovskite equal to 100 nm (b).

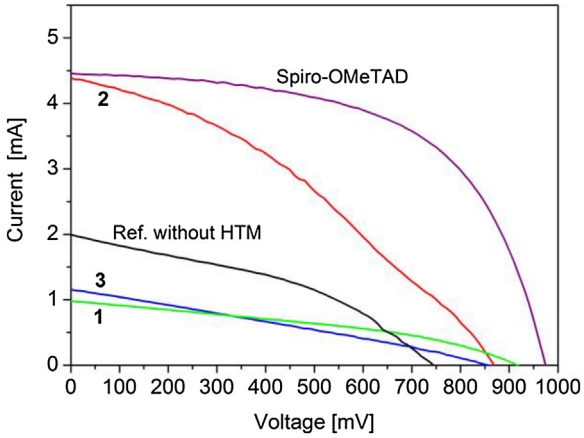

Fig. 6. A comparison of I-V curves of perovskite solar cell with investigated HTMs in comparison with cell without HTM and with Spiro-OMeTAD. The plots were obtained by scanning under 100 mW/cm^2 (1.0 sun) AM1.5 G illumination in forward to reverse direction. The surface of the cells is equal to 0.25 cm^2.

was 4.21 mA, fill factor was 28% and efficiency 4.11%. The lower value of FF indicates a decrease in conductivity while HTM was not doped. Another reason for the worse cell performance than expected may be related to the higher porosity of these layers and the presence of holes, which is caused by the poorer solubility of the tested HTMs (Fig. 6).

4. Conclusions

The investigated compounds are characterized by optimal values of HOMO and LUMO levels, similar to the most commonly used Spiro-OMeTAD. As simulated results showed, the tested molecules can be used in perovskite solar cells and should lead to improvement of their electrical parameters when compared to a reference cell without HTM. This is caused by a decrease in recombination of the perovskite. Nevertheless, in a real experiment, only one of the tested materials bearing four carbazole units (**2**) improved the electrical parameters of the solar cell. An increase in efficiency from 1.60 to 5.31%, V_{oc} from 1.99 to 4.39 V and J_{sc} from 7.96 to 17.56 mA/cm^2 was observed. A drop of FF is the result of obtaining a thin and not defect-free layer and insufficient material conductivity. That can be improved by modification of the chemical structure of the material, as well as the device and the utilization of an optimal dopant that should increase the conductivity.

Author contribution

Katarzyna Gawlińska-Nęcek prepared solar cells and registered photovoltaic parameters, as well as participated in the discussion of the photovoltaic properties and in manuscript preparation.

Zbigniew Starowicz carried out AFM measurement and participated in solar cells investigations.

Daiva Tavgeniene and Gintare Krucaite synthesized and characterized the investigated HTM compounds.

Saulius Grigalevicius designed the compounds and participated in the discussion and manuscript preparation.

Marek Lipiński designed the investigations, carried out the simulation, participated in the discussion and co-produced the manuscript.

Ewa Schab-Balcerzak conceived this study and co-produced the manuscript.

Acknowledgements

DT is obliged for Young Scientists Award from Lithuanian Academy of Science. GK is thankful for a postdoctoral fellowship from Kaunas University of Technology Business Support Fund.

References

[1] H.S. Kim, C.R. Lee, J.H. Im, K.B. Lee, T. Moehl, A. Marchioro, S.J. Moon, R. Humphry-Baker, J.H. Yum, J.E. Moser, M. Grätzel, N.G. Park, Lead iodide perovskite sensitized all-solid-state submicron thin film mesoscopic solar cell with efficiency exceeding 9%, Sci. Rep. 2 (2012) 1–7.
[2] F.A. Roghabadi, N. Ahmadi, V. Ahmadi, A. Di Carlo, K.O. Aghmiuni, A. Shokrolahzadeh, T. Farzaneh, S. Ghoreishi, M. Payandeh, N. Mansour, R. Fumani, Bulk heterojunction polymer solar cell and perovskite solar cell: concepts, materials, current status, and opto-electronic properties, Sol. Energy 173 (2018) 407–424.
[3] M. Nazim, S. Ameen, M.S. Akhtar, M.K. Nazeeruddin, H.-S. Shin, Tuning electronic structures of thiazolo[5,4-d]thiazole-based hole transporting materials for efficient perovskite solar cells, Sol. Energy Mater Sol. 180 (2018) 334–342.
[4] P. Vivo, J.K. Salunke, A. Priimagi, Hole-transporting materials for printable perovskite solar cells, Materials 10 (2017) 1087–1132.
[5] X. Yang, H. Wang, B. Cai, Z. Yu, L. Sun, Progress in hole-transporting materials for perovskite solar cells, J. Energy Chem. 27 (2018) 650–672.
[6] X. Zhao, M. Wang, Organic hole-transporting materials for efficient perovskite solar cells, Mater. Today Energy 7 (2018) 208–220.
[7] Z.-U. Rehman, A. Saeed, M. Faisal, Synthesis and characterization of thiophene-mediated hole transport materials for perovskite solar cells, Synth. Met. 214 (2018) 54–68.
[8] P. Agarwala, D. Kabra, A review on triphenylamine (TPA) based organic hole transport materials (HTMs) for dye sensitized solar cells (DSSCs) and perovskite solar cells (PSCs): evolution and molecular engineering, J. Mater. Chem. A 5 (2017) 1348–1373.
[9] K. Gawlinska, A. Iwan, Z. Starowicz, G. Kulesza-Matlak, K. Stan-Glowinska, M. Janusz, M. Lipinski, B. Boharewicz, I. Tazbir, A. Sikora, Searching of new, cheap, air- and thermally stable hole transporting materials for perovskite solar cells, Opto-Electron. Rev. 25 (2017) 274–284.
[10] R. Rajeswari, M. Mrinalini, S. Prasanthkumar, L. Giribabu, Emerging of inorganic hole transporting materials for perovskite solar cells, Chem. Rec. 17 (2017) 681–699.
[11] C. Chen, W. Zhang, J. Cong, M. Cheng, B. Zhang, H. Chen, P. Liu, R. Li, M. Safdari, L. Kloo, L. Sun, Cu(II) Complexes as p-type dopants in efficient perovskite solar cells, ACS Energy Lett. 2 (2017) 497–503.
[12] X. Yang, H. Wang, B. Cai, Z. Yu, L. Sun, Progress in hole-transporting materials for perovskite solar cells, J. Energy Chem. 27 (2018) 650–672.
[13] D. Tavgeniene, L. Liu, G. Krucaite, D. Volyniuk, J.V. Grazulevicius, Z. Xie, B. Zhang, S. Grigalevicius, Phenylvinyl-substituted carbazole twin compounds as efficient materials for the charge-transporting layers of OLED devices, J. Electron. Mater. 44 (2015) 4006–4011.
[14] X.-F. Zhang, C. Liu, L. Zhang, J. Wu, B. Xu, Triazatetrabenzcorrole (TBC) as efficient dopant-free hole transporting materials for organo metal halide perovskite solar cells, Dye. Pigment. 137 (2017) 208–213.
[15] V. Vaitkeviciene, A. Kruzinauskiene, S. Grigalevicius, J.V. Grazulevicius, R. Rutkaite, V. Jankauskas, Well-defined [3,3']bicarbazolyl-based electroactive compounds for optoelectronics, Synth. Met. 158 (2008) 383–390.
[16] H. Xu, P. Sun, K. Wang, X. Zhang, J. Ren, T. Yang, X. Zhang, Y. Hao, H. Wang, B. Xu, W.-Y. Wong, Solution-processed blue and blue-green phosphorescent organic light-emitting devices using iridium(III) complexes based on 9-(6-(4-phenyl-1H-1,2,3-triazol-1-yl)hexyl)-9H-carbazole ligand, Dye. Pigment. 134 (2016) 148–154.
[17] R. Griniene, L. Liu, D. Tavgeniene, D. Sipaviciute, D. Volyniuk, J.V. Grazulevicius, Z. Xie, B. Zhang, K. Leduskrasts, S. Grigalevicius, Polyethers with pendent phenylvinyl substituted carbazole rings as polymers for hole transporting layers of OLEDs, Opt. Mater. 51 (2016) 148–153.
[18] M. Burgelman, P. Nollet, S. Degrave, Modelling polycrystalline semiconductor solar cells, Thin Solid Films 361–362 (2000) 527–532.
[19] E. Miyamoto, Y. Yamaguchi, M. Yokoyama, Denshishashin Gakkai-shi (Electrophotography), 28, 1989, pp. 364.
[20] N.A. Kukhta, D. Volyniuk, L. Peciulyte, J. Ostrauskaite, G. Juska, J.V. Grazulevicius, Structure–property relationships of star-shaped blue-emitting charge-transporting 1,3,5-triphenylbenzene derivatives, Dye. Pigment. 117 (2015) 122.
[21] S. Agarwal, P.R. Nair, Device engineering of perovskite solar cells to achieve near ideal efficiency, Appl. Phys. Lett. 107 (2015), 123901.